# Dynamics of cloudy boundary layers

**Peter G. Duynkerke**

*Utrecht University*
*Institute for Marine and Atmospheric Research Utrecht (IMAU)*
*The Netherlands*

**ABSTRACT**

Cloud-topped boundary layers with stratocumulus and cumulus are a dominant feature of the climate system over extensive areas of the globe. The dominant physical processes in such a boundary layer are described. Attention is given to the most important processes affecting turbulence, and in particular entrainment at cloud edges. The parametrization of cumulus and stratocumulus-topped boundary layers with a mass-flux approach is discussed.

## 1. Introduction

The presence of boundary clouds leads to considerable complications in the turbulence structure compared to a clear atmospheric boundary layer (ABL) because of the important role played by phase changes and radiative fluxes. In the clear ABL the mean variables, the turbulent structure and their time evolution are mainly controlled by large-scale external conditions and by the surface fluxes. In a cloudy ABL, the surface fluxes may be important, but phase changes and radiative fluxes produce local sources of heating (or cooling) within the interior of the ABL and therefore can greatly influence its turbulent structure and dynamics. Therefore, the presence of cloud has a large impact on boundary layer structure and upon surface weather. The cloud-topped boundary layer is limited in the vertical by the main capping inversion or subsidence and consists of two main cloud types: stratocumulus and cumulus.

The turbulent and thermodynamical structure of stratocumulus has been thoroughly studied from measurements; see review by Driedonks and Duynkerke (1989), Hignett (1991), Paluch and Lenschow (1991), Duynkerke et al. (1995), Albrecht et al. (1995), Roode and Duynkerke (1997). Until now mainly observations have revealed the importance of the different physical processes for the dynamics of stratocumulus. However, in the future we will rely more often on 3-dimensional Large Eddy simulations (LES) to reveal the detailed structure of these layered clouds.

The in-cloud turbulence dynamics of shallow cumulus has been studied and documented much less than the stratocumulus counterpart. Important in-cloud observational studies are Warner (1977), Jonas (1990), Blyth (1993), Roode and Duynkerke (1995), Smith and Jonas (1995) and Grinnell et al. (1996). Here there is a reasonable balance between LES studies (Sommeria, 1976; Cuijpers and Duynkerke, 1993; Siebesma and Cuijpers, 1995) and field experiments. However it is amazing that, compared to stratocumulus, from observations so little is known about the detailed in-cloud turbulence and thermodynamical structure.

Important scaling parameters and parametrizations for the dynamics of shallow convective clouds will be discussed in section 2. In the sections 3 and 4 an attempt is made to summarise the structure and dynamics of the cloud-topped boundary layer for stratocumulus and cumulus, respectively.

# 2. Boundary layer scaling and parametrizations

## 2.1 Local Scaling

For steady state conditions and in case we can neglect the turbulent transport and subsidence terms the turbulent kinetic energy (TKE) equation reduces to:

$$0 = -\overline{u'w'}\frac{\partial \overline{u}}{\partial z} - \overline{v'w'}\frac{\partial \overline{v}}{\partial z} + \frac{g}{\theta_0}\overline{w'\theta_v'} - \varepsilon . \qquad (2.1)$$

Equation (2.1) states that the kinetic energy budget is completely determined by local parameters. In that case we can express the fluxes in terms of their local gradients using the turbulent exchange coefficient $K_m$ :

$$\left(\overline{u'w'}, \overline{v'w'}\right) = - K_m \left(\partial\overline{u}/\partial z, \partial\overline{v}/\partial z\right) \qquad (2.2)$$

With the definition $\tau = \left(\overline{u'w'}^2 + \overline{v'w'}^2\right)^{1/2}$ and multiplying (2.1) with $\kappa z/\tau^{3/2}$ we obtain:

$$0 = \phi_m + z/\Lambda - \phi_\varepsilon ,$$
$$\text{with: } \phi_m = \frac{\kappa z}{\tau^{1/2}}\left((\partial\overline{u}/\partial z)^2 + (\partial\overline{v}/\partial z)^2\right)^{1/2} , \ \Lambda = \frac{\tau^{3/2}}{\kappa\, g/\theta_0\, \overline{w'\theta_v'}} , \ \phi_\varepsilon = \frac{\kappa z}{\tau^{3/2}}\varepsilon . \qquad (2.3)$$

This equation states that the local dimensionless wind shear and dissipation only depend upon the stability parameter z/Λ. This is the most general form of local scaling and is used in the stable and neutral (Grant 1992) boundary layer and the surface layer.

## 2.2 Convective Scaling

Local scaling is not appropriate in unstable conditions above the surface layer since the structure of turbulence is insensitive to τ but buoyancy effects dominate, and the boundary layer depth h becomes now the dominant (external) length scale. This can be understood from the TKE budget by recognising that the transport term (T) in the TKE equation becomes of similar order as the buoyancy production. This means that the mixed layer scaling involves the convective velocity and temperature scales $w_*$ and $T_*$, respectively:

$$w_*^3 = g/\theta_0 \left(\overline{w'\theta_v'}\right)_s h$$
$$T_* = \left(\overline{w'\theta_v'}\right)_s / w_* \qquad (2.4)$$

so that non dimensional properties are functions of z/h alone. A commonly used parameter to indicate the stability of the boundary layer is h/L.

For the cloud-topped boundary layer no general scaling is available because the buoyancy flux is not a simple universal function of height as in the clear convective ABL. Therefore a generalised convective velocity scale was typically used which, instead of only the surface buoyancy flux, depends on the buoyancy flux integrated over the whole boundary layer depth:

$$w_*^3 = c \int_{h_m}^{h} g/\theta_0 \, \overline{w'\theta_v'} \, dz \,, \qquad (2.5)$$

The constant is fixed by the fact that for the dry convective ABL (2.5) reduces to (2.4). This gives for $h_m = 0$ and a typical entrainment flux at the boundary layer height (h)

$$\left(\overline{w'\theta_v'}\right)_h = -\,0.2\,\left(\overline{w'\theta_v'}\right)_s \qquad (2.6)$$

a value of $c = 2.5$ in (2.5).

### 2.3 Entrainment

In the upper part of the mixed layer there is an exchange of air from the free troposphere with boundary layer air. In this case we describe the inversion as a discontinuity with jump properties $\Delta$, where $\Delta$ stands for the difference of u, v, $\theta_v$, $q_t$ etc. just above and below the inversion. The time evolution of the inversion height is given by

$$\frac{\partial h}{\partial t} = -\,\overline{u}\frac{\partial h}{\partial x} - \overline{v}\frac{\partial h}{\partial y} + w_e + \overline{w}_h \,, \qquad (2.7)$$

where (u, v) are the horizontal velocities in the (x,y) direction, $w_h$ the large scale vertical velocity and $w_e$ is the entrainment velocity defined by:

$$w_e = -\left(\overline{w'\psi'}\right)_h / \Delta\psi \,, \qquad (2.8)$$

where $\psi$ stands for u, v, $\theta_v$, $q_t$ etc. For the clear convective boundary layer it is observed that the entrainment velocity scales with w* and h:

$$w_e/w_* = 0.2\, Ri_{w*}^{-1} \quad \text{with: } Ri_{w*} = \frac{g/\theta_o \, \Delta\theta_v \, h}{w_*^2} \qquad (2.9)$$

Equation (2.9) together with (2.8) for $\psi = \theta_v$ is identical to the relationship (2.6). For the cloud-topped ABL a relationship similar to (2.9) is still unknown. Several proposals have been made for the case in which the inversion becomes unstable due to evaporative cooling (Deardorff, 1980; Randall, 1980; Siems et al. 1990; MacVean and Mason, 1990; Duynkerke, 1993) and scaling laws are now being proposed. For stratocumulus we will come back to this in section 3.3.

### 2.3 Mass flux approach

In a mass-flux approach the entire atmosphere is divided into 'updrafts' (this can be based on vertical velocity alone or more restrictive conditions) and 'environment' and the average values of quantities like temperature and moisture are calculated for both updrafts and environment. Using the mass-flux approach one can derive a number of exact equations (e.g. Randall et al, 1992). The average values for the entire layer are written as:

$$\overline{\psi} = \sigma\psi_u + (1-\sigma)\psi_e \qquad (2.10)$$

in which $\psi_{u,e}$ are the average values of a quantity $\psi$ for the updraft and environment respectively and $\sigma$ is the updraft area fraction. The vertical turbulent fluxes of a quantity $\psi$ can be written as:

$$F_{\psi m} = M_c(\psi_u-\psi_e) \approx C\ (\rho_0\overline{w'\psi'}) \qquad (2.11)$$

with $\rho_0$ the air density, C the ratio of the flux from the mass-flux approach and the real (measured) flux, $F_{\psi m}$ the flux of the scalar $\psi$ in the mass-flux approach, and $M_c$ the mass flux defined as:

$$M_c \equiv \rho_0\ \sigma\ (w_u-\overline{w}) = \rho_0\ \sigma\ (1-\sigma)\ (w_u - w_e). \qquad (2.12)$$

Equation (2.11) is an important result of this approach; the fluxes of a certain scalar are proportional to the difference between the average values of the scalar for the updraft and the environment.

Mass-flux approaches have been applied successfully to cumulus convection (Betts, 1973; Arakawa and Schubert, 1974). These approaches have proved quite successful in representing shallow cumulus convection and as a result a mass-flux scheme is often used in weather forecast models (for example ECMWF forecast model; Tiedtke, 1989). The mass-flux approach has been analysed from large eddy simulations (LES) for several different types of boundary layers; stratus (Schuman and Moeng, 1991), stratocumulus (Randall et al., 1992) and the dry convective boundary layer (Wyngaard and Moeng, 1992). Wyngaard and Moeng (1992) also compared their LES results with mathematical calculations. Moreover, several observational analyses have been performed following the mass-flux approach (Randall et al. 1992 for an overview; DeLaat and Duynkerke, 1998).

An important process in the convective boundary layer (CBL) is the process of lateral entrainment. When an air parcel is rising or sinking through the boundary layer, it will exchange mass and other quantities like (potential temperature and moisture) with the surrounding air. The mass flux equations (Tiedtke, 1989; Siebesma and Cuijpers, 1995) can be written as:

$$\rho_0 \frac{\partial\sigma}{\partial t} = -\frac{\partial M_c}{\partial z} + E_c - D_c \qquad (2.13)$$

$$\rho_0 \frac{\partial\,\sigma\psi_u}{\partial t} = -\frac{\partial(M_c\psi_u)}{\partial z} + (E\psi_e - D\psi_u) \qquad (2.14)$$

$$\rho_0 \frac{\partial\,(1-\sigma)\psi_e}{\partial t} = \frac{\partial(M_c\psi_e)}{\partial z} + (D\psi_u - E\psi_e) \qquad (2.15)$$

in which E (and $E_c$) represents the entrainment of mass into an updraft and D (and $D_c$) represents the detrainment of mass from the updraft. Note that $E_c$ and $D_c$ in the continuity equation are in general different from those in the scalar equation (Siebesma, 1996; Siebesma and Holtslag, 1996)

# 3. Stratocumulus-topped boundary layer

## 3.1 Processes

The major physical processes that influence the structure of stratocumulus are depicted in Figure 1. Briefly, longwave radiative cooling at cloud top drives the turbulent mixing throughout the boundary layer. This cloud-top cooling supports a positive vertical buoyancy flux throughout the boundary layer and maintains this layer in a well-mixed state. The vertical extent of the radiative cooling, however, is limited to a shallow region, perhaps only a few tens of meters deep adjacent to the top of the cloud. Besides the longwave cooling the surface fluxes can also generate turbulence in the boundary layer. Due to the turbulent kinetic energy in the boundary layer, air is mixed from above the inversion into the boundary layer; a process called entrainment. The entrained air from above the inversion is typically warmer and dryer than the air in boundary layer and therefore

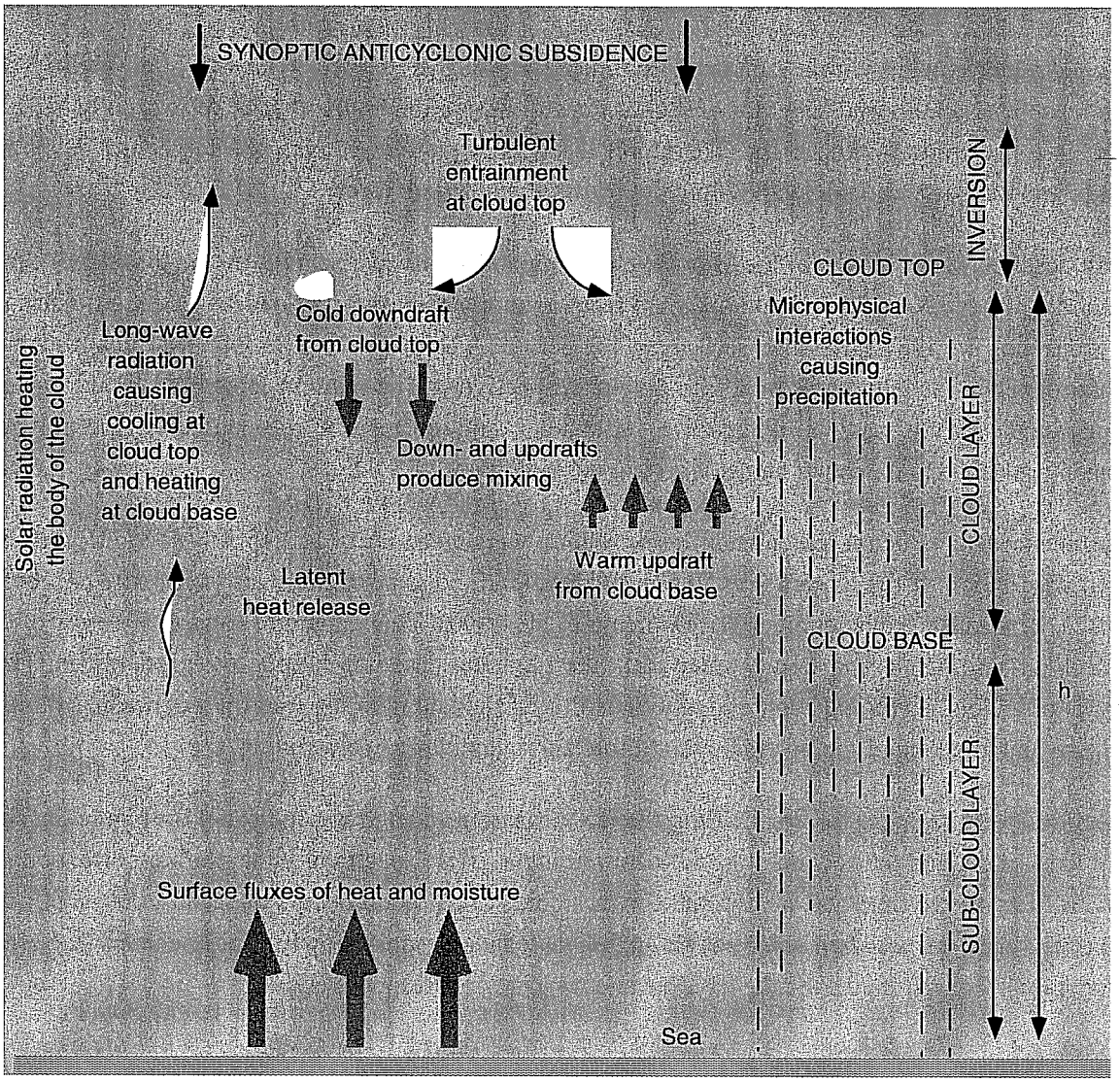


*Figure 1: Summary of physical processes important for the development of stratocumulus (from Nieuwstadt and Duynkerke, 1996).*

entrainment is potentially a mechanism for thinning of the cloud layer. Near cloud base, since the ground temperature is usually a few degrees higher than cloud temperature, the longwave radiation typically causes a slight warming. Due to condensation of vapor there is a latent heat release, which gives a heating in the cloud layer and as such is an additional source for buoyant production of turbulence. During the daytime, solar radiation will influence the cloud by its differential absorption. Because the shortwave heating extends much deeper into the cloud the combined effect of shortwave heating and longwave cooling may lead to a destabilization of the cloud layer itself, and to a decoupling of the cloud layer from the sub-cloud layer. When decoupling occurs the cloud would be cut off from the moisture input from the surface, which would lead to a rapid thinning of the cloud layer, resulting in breaking up or at least a marked diurnal cycle.

The longwave radiative cooling at cloud top will generate convective instability. This instability is removed by turbulent motions which are observed to take the form of cold downdrafts descending from the vicinity of the cloud top, with associated warm compensating updrafts. Thus cold air is brought down further into the cloud from the cloud top while warm air ascends.

The liquid water content within stratocumulus increases roughly linearly with height at slightly below the adiabatic value (Nicholls and Leighton, 1986). Aircraft observations show that there is usually little variation in droplet concentration with height. Therefore, the deeper the cloud layer, the larger the drops that form within it, and there is a critical depth (about 300m) at which drizzle forms.

We will describe the influence of the longwave cooling and shortwave heating on the turbulence structure of the boundary layer. We will use data obtained from a comprehensive array of surface-based instrumentation deployed during the 1987 FIRE intensive observing period. A Doppler acoustic sounder and a laser ceilometer measured inversion height and cloud base height, respectively. The column integrated liquid water content was measured with a passive microwave radiometer and turbulence measurements were made using instruments attached to the tether cable of a 1076 $m^3$ balloon.

The turbulence data to be presented later in this section were taken on 14 and 15 July 1987 (Hignett, 1991). A detailed description of the temporal evolution of the cloud cloud conditions on 14/15 July can be found in Figure 2 (see also Blaskovic et al., 1991; Albrecht et al., 1990). This diagram shows time series of cloud-top height, cloud-base height and liquid water path; the plots are based on hourly-averaged values. The overall picture is of a cloud layer that progressively thins during the late morning into the afternoon, both by raising cloud base and lowering of the inversion, but it thickens again during the evening.

Two periods were selected for detailed turbulence measurements and are indicated on Figure 2. The first is around local noon, and the second close to local midnight. More specifically the periods correspond to 1830-2100 UTC for the daytime and 0530-0800 for the night. Local noon occurs at about 2000 UTC; hence the daytime data were taken when solar zenith angle was changing only slowly. The boundary layer height (h) was about 604m and 570m during the daytime and night period, respectively.

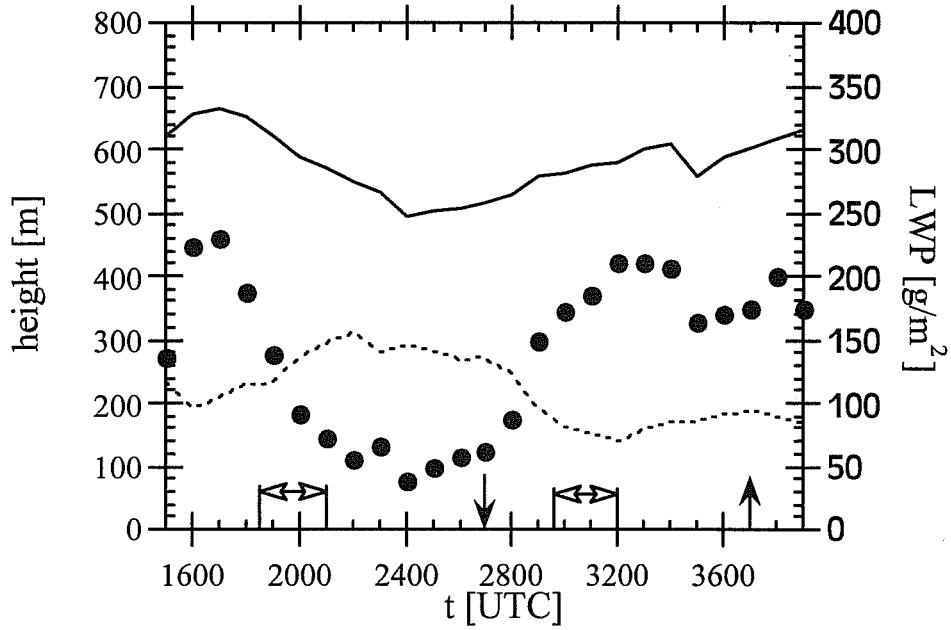


*Figure 2: Liquid water path, LWP, (•) and height of cloud top (full line) and cloud base (dashed line) against time from 1500 UTC 14 July to 1500 UTC 15 July 1987. All data are hourly averaged values. The horizontal arrows denote the periods selected for detailed measurements. Vertical arrows denote sunset (↓) and sunrise (↑).*

## 3.2 Scaling

The vertical velocity variance is used as an indicator of the convective activity and is plotted against normalised height on Figure 3a for the day and night period. This Figure also shows the range of cloud base heights measured by the ceilometer during theses periods (about 267m and 156m). The daytime vertical velocity variance profile shows the typical low values above cloud, a distinct maximum in the cloud layer and evidence of a second weak maximum below the cloud. This profile is similar to that shown by Nicholls (1984) and is consistent with mixing being driven from the surface and cloud top. The nocturnal data have the appearance of a more intensely turbulent layer well mixed from the inversion to the sea surface. Driven by longwave cooling from cloud top in a manner analogous to that of a convective boundary layer heated from below (Lenschow et al., 1980).

These features are also reflected in the behaviour of the buoyancy flux (Figure 14 in Nieuwstadt and Duynkerke, 1996). In both cases, the profiles tend to a weak positive surface flux and flux maxima located close to cloud top. It is clear that the larger buoyancy fluxes occur at night and this leads to the more intensely turbulent layer observed during this period. Whereas the nocturnal data give the appearance of a single mixed layer driven by cloud-top longwave cooling, the daytime buoyancy profile has a distinct minimum value around cloud-base height. From turbulent length scale estimates Hignett (1991) concluded that the daytime boundary layer revealed two distinct layers: the cloud and sub-cloud layer. Moreover, from a modelling simulation of this case Duynkerke and Hignett (1993) found that the buoyancy flux at cloud base was actually slightly negative, which give rise to the formation of a slightly stable layer and as a consequence a decoupling

of the cloud layer from the sub-cloud layer. The decoupling is a consequence of the shortwave heating in the cloud layer. The shortwave heating is about as large as the longwave cooling, but is distributed over a thicker layer near cloud top, and together with the entrainment of warm air leads to a negative buoyancy at cloud base. This decoupling has a marked influence on the diurnal variation in the cloud layer.

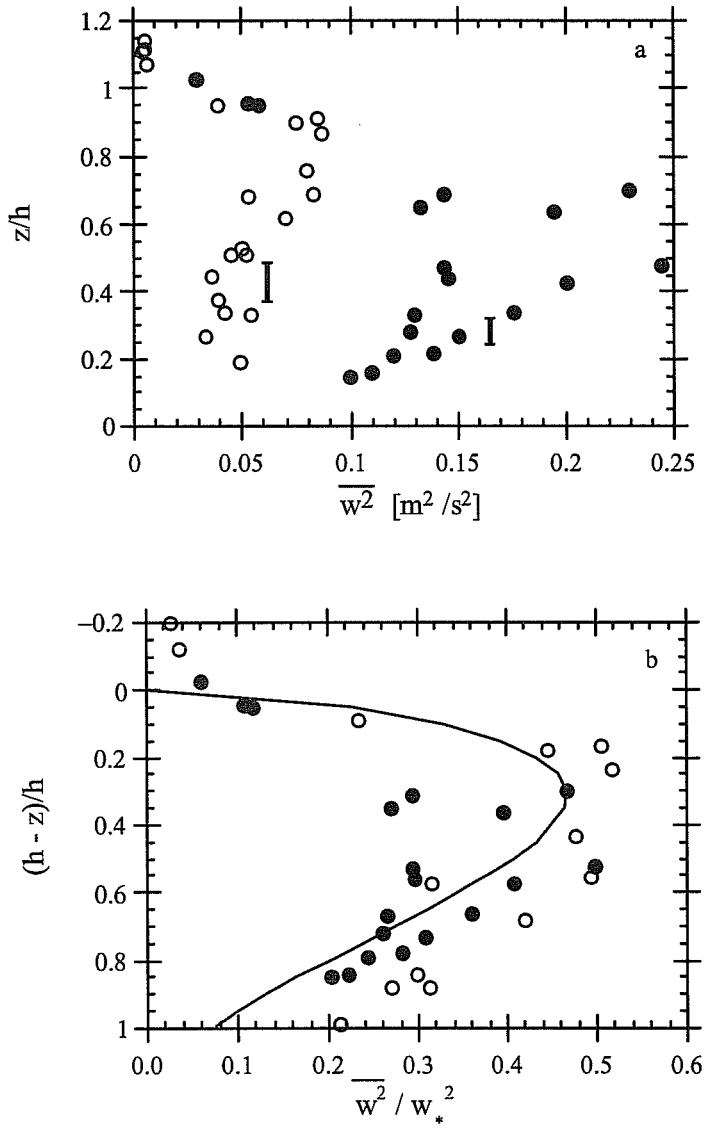


*Figure 3: a) Vertical velocity variance against normalised height for the daytime (open circles) and night-time period (full dots). The vertical bars indicate the range of cloud base height during each period. b) Vertical velocity variance (normalised with the convective velocity scale w*) against distance from cloud top (normalised with the mixed layer depth) for the daytime (open circles) and night-time period (full dots). The line is from Lenschow et al. (1980), plotted upside down.*

The daytime cloud layer and complete nocturnal boundary layer are thus examples of convectively driven mixed layers. Although it is unlikely that a universal law is applicable to cloudy convective layers we will apply the approach proposed in section 2.2. In that approach $w_*^3$ is equal to 2.5 times the integral of the buoyancy flux in the mixed layer. For the nocturnal data the mixed layer depth is the full depth of the boundary layer and for the daytime data its is the depth of the cloud layer. Which gives a value of 0.4 and 0.7

for the daytime and night period, respectively. The resulting scaled mixed-layer variances are plotted in Figure 3b with a curve derived by Lenschow et al. (1980) (and plotted upside down) from measurements in the convective boundary layers over land. The overall scatter is quite large but shows a similar structure to the scaled vertical velocity variance for five different cases shown by Nicholls (1989).

Turbulence in the stratocumulus-topped boundary layer can also be dominated by shear in those cases the typical convective structures of stratocumulus are absent, and a better name for this type of cloud would be stratus. The wind shear (Brost et al. 1982 a,b; Nicholls and Leighton, 1986) can be quite strong under high wind speed or baroclinic conditions. Measurements indicate that wind shear at cloud top generated turbulence locally, promoting entrainment of warmer air from above the inversion. This entrainment approximately balanced the cloud top radiative cooling. The turbulence structure strongly resembles the near-neutral, shear-dominated mixed layers. Probably the idea of local similarity (section 2.1) can be used to scale the structure of turbulence as in the cloud free near-neutral boundary layer (Grant, 1992).

### 3.3 Dynamics: Decoupling and Entrainment

As summarised in the introduction there are many physical processes that influence the dynamics of a stratocumulus-topped boundary layer and as such a complete treatment is outside the scope of this paper. Here we will mainly concentrate on two aspects: decoupling and entrainment. The decoupling of the cloud layer from the sub-cloud layer leads to two turbulent layers between which there is only limited turbulent exchange. Besides the influence on the turbulence structure of the boundary layer the decoupling has also important consequences for the dynamics of the cloud layer. The formation of a slightly stable layer near cloud base prevents the moisture to be transported upwards from the sea surface into the cloud layer. This together with the solar heating leads to a rapid thinning of the cloud layer during daytime. It can be seen from Figure 2 that this is due to the decoupling the cloud layer progressively thins during the late morning and into the afternoon. Although it did not break completely it became very thin around 2400 UTC and is very transparent for solar radiation (transmission of about 50%). The rapid thinning of the cloud layer as a result of decoupling therefore has important influence on the radiation balance both at the surface and above the cloud and as a consequence this can have an important impact on weather and climate simulations.

Because extensive marine stratocumulus clouds are a persistent feature of the eastern parts of the major ocean basins it is obvious that the inversion height must be almost stationary and therefore there must be a close balance between the entrainment velocity and subsidence velocity at cloud top (2.7). The subsidence velocity is mainly determined by large scale processes whereas the entrainment velocity is governed by the turbulence intensity in the boundary layer and the strength of the inversion, as discussed in section 2.3. Therefore given the subsidence velocity the entrainment velocity will determine the final depth of the boundary layer. For the clear convective boundary layer it was found that the scaled entrainment velocity is a function of $Ri_{w*}$ only (2.9). If we use observations of the entrainment velocity (Nicholls and Turton, 1986; Roode and Duynkerke, 1997) and scale them analogous to (2.9) we obtain that the constant is about 2 instead of 0.2 (Figure 4). From this we can conclude that (2.9) is not a generally valid (A constant) parametrization for entrainment in convective boundary layers.

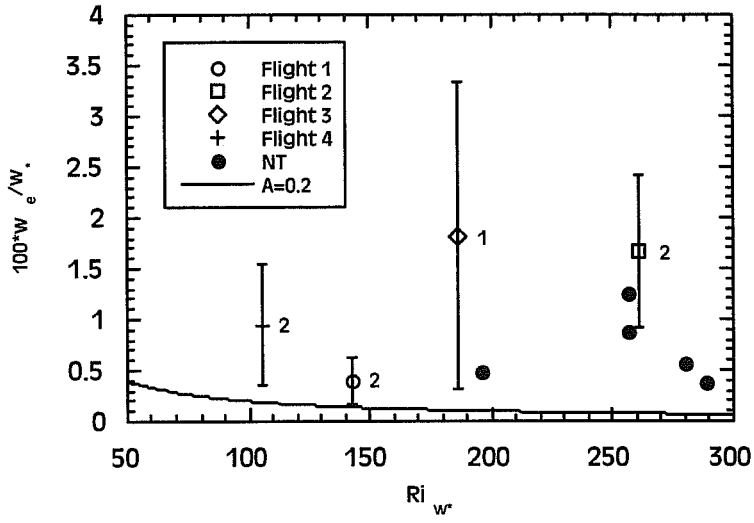


*Figure 4: The entrainment velocity normalised by the convective velocity scale (w*) as a function of the Richardson number ($Ri_{w*}$): from the first Lagrangian of ASTEX (Roode and Duynkerke, 1997) and 'NT' (Nicholls and Turton, 1986) and theoretical relationship for the clear convective boundary layer (A = 0.2).*

This difference in A might also be a consequence of the fact that we have used $\Delta\theta_v$ to denote the strength of the inversion in the definition of $Ri_{w*}$. But $\Delta\theta_v$ does not take into account the effect of evaporative cooling on the entrainment process and therefore an additional parameter has to be added to the list of parameters to scale the entrainment velocity (Nicholls and Turton, 1986; Siems et al., 1990; MacVean and Mason, 1990; Duynkerke, 1993). This is still an area of active research where more observational data and modelling studies are required to verify present theories.

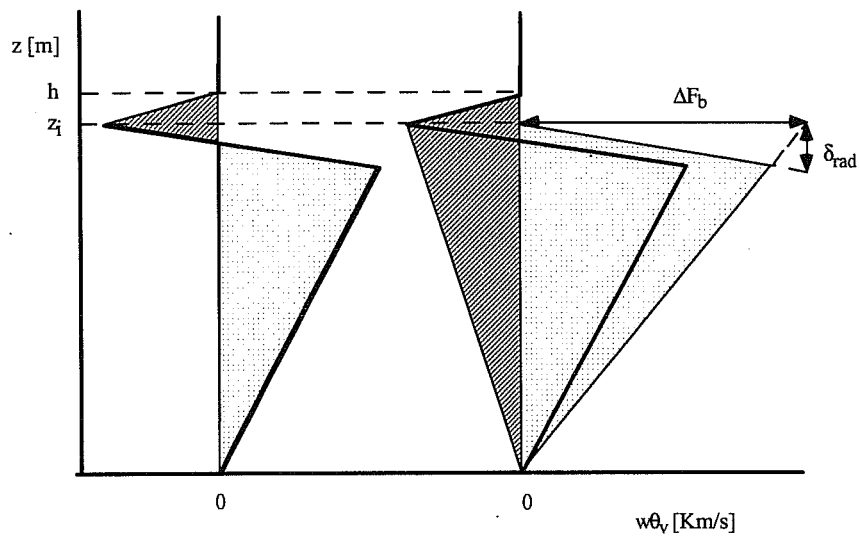


*Figure 5: The productive part (dots) and the consumptive part N (solid lines) of the buoyancy flux (thick line) for the smoke boundary layer; Eulerian (left) and process partitioning (right). $\Delta F_b$ is the radiative flux divergence in the boundary layer below $z_i$ that takes place over a vertical distance $\delta_{rad}$.*

Recent papers discussing the different scaling laws of the entrainment velocity are Lock (1998), VanZanten et al. (1998) and Moeng (2000). In VanZanten et al. (1998) three different entrainment parametrization are tested: Eulerian partitioning (ep), process partitioning (pp) and convective scaling (cs). It was concluded that the convective scaling parametrization (2.9) of the entrainment velocity did not work for the stratocumulus (see also above). The Eulerian and process partitioning both assume that the buoyancy flux consists of a TKE producing (P) and consuming (N) part. In the Eulerian partitioning the producing (consuming) part is the integral of the positive (negative) buoyancy flux. Whereas, in the process partitioning it is assumed that each process (surface buoyancy flux, radiation, entrainment, etc.) apart contributes either to production or consumption of TKE. For the smoke boundary layer with zero surface buoyancy flux this is schematically shown in Figure 5. For this type of boundary layer an analytical solution for the entrainment buoyancy flux was obtained for the two closures (ep and pp). These are compared with Large Eddy Simulations (Figure 6) from which it is concluded that the process partitioning agrees best with LES results in the limit $\delta_{rad}/z_i \rightarrow 0$.

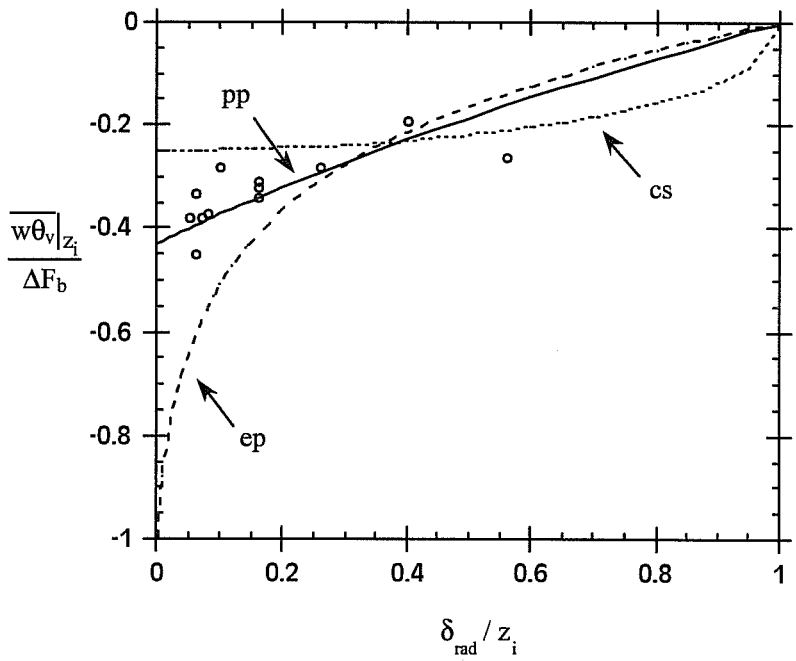


*Figure 6: Analytical relations between the dimensionless entrainment flux* $\overline{w\theta_v}|_{z_i} / \Delta F_b$ *and dimensionless depth* ($\delta_{rad}/z_i$) *over which the radiative cooling takes place for a smoke boundary layer with zero surface buoyancy flux: Eulerian partitioning (ep), process partitioning (pp) and convective scaling (cs) according to (2.9). Results from a Large Eddy Simulation are shown as circles (Van Zanten et al., 1998).*

## 4. Cumulus

Shallow cumulus clouds are found on many locations around the world, with a globally averaged cloud amount of 12% and 5% over ocean and land, respectively. Large areas of cumulus clouds exist in the trade-wind regions and over the mid-latitude continents in summer. These cumulus clouds are important for the large-scale atmospheric dynamics because of their vertical transport of heat, moisture and momentum.

Cumulus clouds act to couple the boundary layer to the free troposphere through the transport of heat, moisture and momentum, as well as pollutants, through the inversion. No scaling laws (section 2.2) are available for the turbulence structure of shallow cumulus; as such each case needs a new plot (with dimensions!).

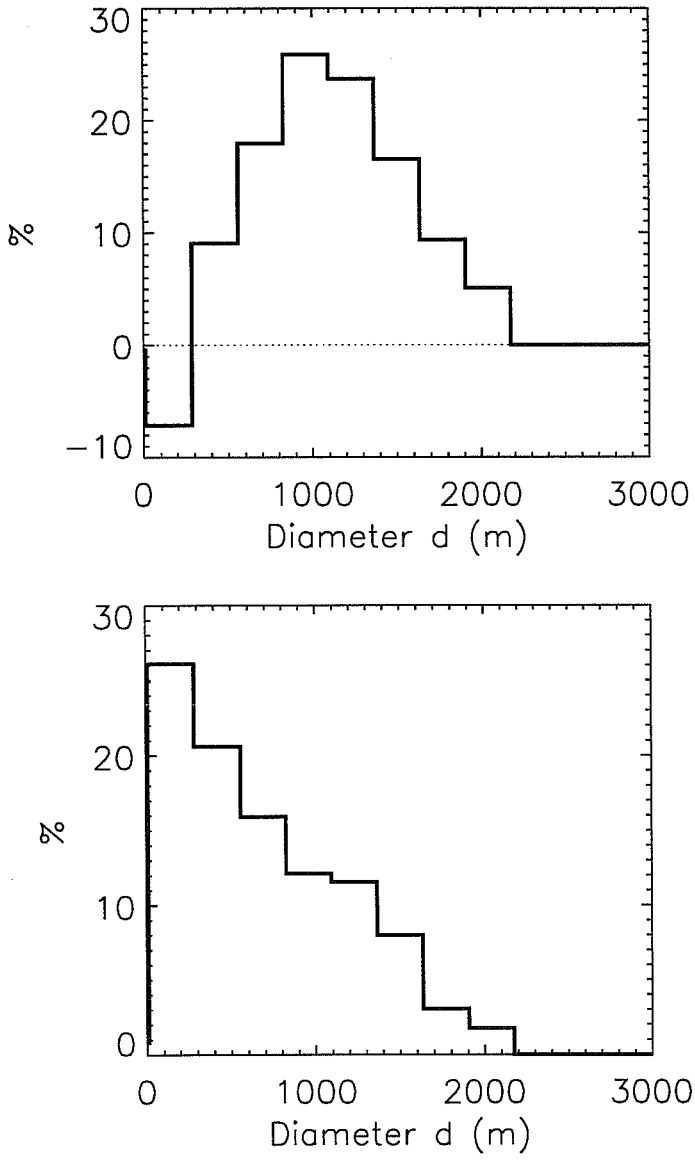


*Figure 7: In percentage the number distribution (lower) and the contribution to the mass-flux (upper) as a function of cumulus cloud size.*

We have also analysed the thermodynamical properties of the cloud and the environment. At a certain height the average in-cloud and environmental values for liquid water, water vapor, potential temperature, mass flux, etc. are calculated. The values obtained for liquid and total water content are shown in Figure 8. In this Figure also the adiabatic liquid water content (2.2 g/kg/km) is shown together with the total water content measured during a profile flight. The in-cloud total water content is typically 2.4 g/kg higher than in the environment, almost independent of height. Assuming the cloud fraction small ($\sigma << 1$) we obtain from (2.14) for the total water content ($q_t$):

$$\frac{\partial q_{t,c}}{\partial z} = \varepsilon (q_{t,e} - q_{t,c}) \qquad (4.1)$$

The gradient of the in-cloud total water content ($q_{t,c}$) is about –3.0 g/kg/km that gives a typical value of $\varepsilon \approx 1.2 \times 10^{-3}$ m$^{-1}$. This value of $\varepsilon$ is close to the one obtained by Siebesma and Cuijpers (1995) from an LES based on BOMEX. From the continuity equation (2.13) also the detrainment was determined which gave a value of $\delta \approx 4 \times 10^{-4}$ m$^{-1}$. The value of $\varepsilon$ is much larger than the value used in mass flux schemes used in global circulation models (see for a discussion Siebesma and Cuijpers, 1995; Siebesma and Holtslag, 1996) and therefore a better theoretical understanding of the lateral entrainment rates is needed.

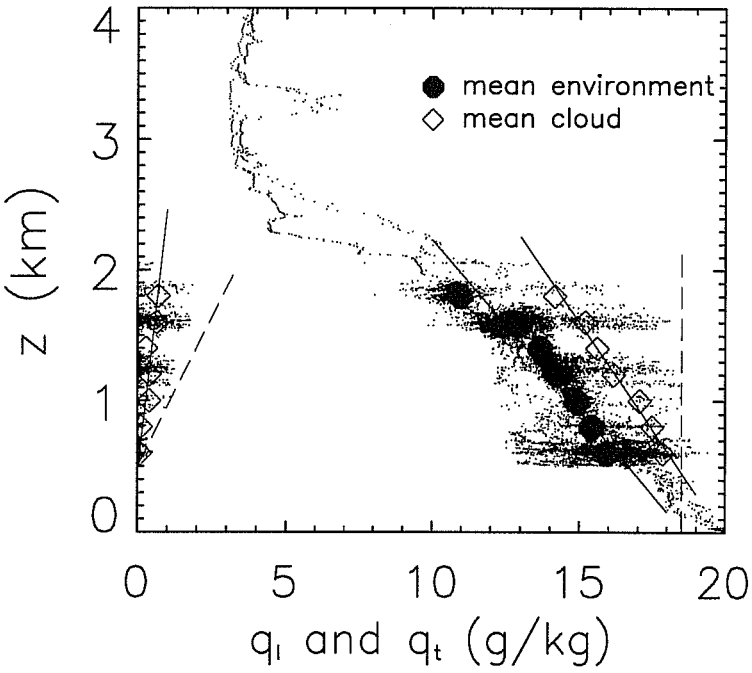


*Figure 8: Horizontally averaged liquid water content (diamonds on the left) and total water content (inside cloud: diamonds; outside cloud: full circles) as a function of height. The dotted line up to 4km displays the liquid water and total water content measured during a profile flight. The dashed lines represent an undiluted (adiabatic) parcel ascent: adiabatic liquid water content and constant total water content.*

Similar to Warner (1977) we analysed the in-cloud vertical velocity as a function of height and found analogous results: the mean vertical velocity is small (about 1.0 m/s) and shows no systematic variation with height, but the r.m.s. of the fluctuations around the mean shows an almost linear increase with height. The variance of the fluctuations is so large that there is more kinetic energy in the fluctuations than in the mean in-cloud vertical velocity. This indicates that the in-cloud dynamics is complex with strong downdrafts even inside the cloud (Jonas, 1990; Warner, 1977). It is amazing how little quantitative observations there are of the in-cloud cumulus dynamics, in this research area more observations are needed.

## 5. Concluding remarks

The importance of clouds on the radiation budget of the atmosphere and their transport properties makes that the cloud-topped boundary layer will remain a challenging field of research in the future. Topics that need further research are:

A theory is needed which predicts the entrainment velocity in the clear convective boundary layer; the entrainment buoyancy flux is about 25% of the surface buoyancy flux. Further research is needed to understand the dynamics and parametrization of entrainment at the tops of stratocumulus. Important questions are: Which velocity and length scales are important in the entrainment process?, What parameter determines the strength of the inversion ($\Delta\theta_V$, $\Delta_2$, etc.; see Duynkerke, 1993)?; How should we scale the entrainment velocity in different types of convective boundary layers?

As a community we should develop a unique way to define clouds and cloud edges. For instance, the definition could be based on the liquid water content, extinction of radiation, number of droplets, dynamics, etc. Some papers also use the term 'cloud' if it exceeds a certain size (e.g. > 300m). It is desirable to have a common definition such that it is possible to compare observational and model results.

For the parametrization of convective cloudy boundary layers it is necessary to develop a unified mass-flux scheme that can be used in the clear convective boundary layer, stratocumulus and cumulus (Roode et al., 2000). In the latter two cases is desirable to have the same mass-flux scheme in both the cloud and sub-cloud layer. In mass flux schemes it is necessary to have an improved understanding of the scaling of the lateral exchange terms (E and D).

Because of the lack of good in-cloud observations of cumulus dynamics it is necessary to have a field experiment in the cumulus trade wind regions in the near future.

**Acknowledgements**

Dr. C.A. Knight kindly supplied us the data collected by means of the C-130 of NCAR during SCMS. I acknowledge NCAR and its sponsor, the National Science Foundation, for the use of the observational data.

**REFERENCES**

Albrecht, B.A., C.W. Fairall, D.W. Thomson, A.B. White, J.B. Snider and W.H. Schubert, 1990: Surface-based remote sensing of the observed and the adiabatic liquid water content of stratocumulus clouds. *Geophysical Research Letters*, **17**, 89-92.

Albrecht, B.A., C.S. Bretherton, D. Johnson, W.H. Schubert and A.S. Frisch, 1995: The Atlantic Stratocumulus Transition Experiment-ASTEX. *Bull. Amer. Meteor. Soc.*, **76**, 889-904.

Arakawa, A. and W.H. Schubert, 1974: Interaction of a cumulus cloud ensemble with the large-scale environment. *J. Atmos. Sci.*, **31**, 674-701.

Betts, A.K., 1973: Non precipitating cumulus convection and its parametrization. *Quart. J. Roy. Meteor. Soc.*, **99**, 178-196.

Blaskovic, M., R. Davies and J.B. Snider, 1991: Diurnal variation of marine stratocumulus over San Nicolas Island during July 1987. *Mon. Wea. Rev.*, **119**, 1469-1478.

Blyth, A.M., 1993: Entrainment in cumulus clouds. *J. Appl. Meteor.*, **32**, 626-641.

Brost, R.A., D.H. Lenschow and J.C. Wyngaard, 1982a: Marine stratocumulus layers. Part I: Mean conditions, *J. Atmos. Sci.*, **39**, 800-817.

Brost, R.A., J.C. Wyngaard and D.H. Lenschow, 1982b: Marine stratocumulus layers. Part II: Turbulence budgets, *J. Atmos. Sci.*, **39**, 818-836.

Cuijpers, J.W.M. and P.G. Duynkerke, 1993: Large eddy simulation of trade wind cumulus clouds. *J. Atmos. Sci.*, **50**, 3894-3908.

Deardorff, J.W., 1980: Cloud-top entrainment instability. *J. Atmos. Sci.*, **37**, 131-147.

DeLaat, A.T.J., and P.G. Duynkerke, 1998: Analysis of ASTEX-stratocumulus observational data using a mass flux approach. *Boundary-Layer Meteor.*, **86**, 63-87.

Driedonks, A.G.M. and P.G. Duynkerke, 1989: Current problems in the stratocumulus-topped atmospheric boundary layer. *Boundary-Layer Meteor.*, **46**, 275-304.

Duynkerke, P.G., 1993: The stability of cloud top with regard to entrainment: amendment of the theory of cloud-top entrainment instability. *J. Atmos. Sci.*, **50**, 495-502.

Duynkerke, P.G. and P. Hignett, 1993: Simulation of diurnal variation in a stratocumulus-capped marine boundary layer during FIRE. *Mon. Wea. Rev.*, **121**, 3291-3300.

Duynkerke P.G., H. Zhang and P.J. Jonker, 1995: Microphysical and turbulent structure of nocturnal stratocumulus as observed during ASTEX. *J. Atmos. Sci.*, **52**, 2763-2777.

Grant, A.L.M., 1992: The structure of turbulence in the near neutral atmospheric boundary layer. *J. Atmos.Sci.*, **49**, 226-239.

Grinnell, S.A., C.S. Bretherton, D.E. Stevens and A.M. Fraser, 1996: Vertical mass flux calculations in Hawaiian trade cumulus clouds from dual-doppler radar. *J. Atmos. Sci.*, **53**, 1870-1886.

Hignett, P., 1991: Observations of the diurnal variation in a cloud-capped marine boundary layer. *J. Atmos Sci.*, **48**,1474-1482.

Jonas, P.R., 1990: Observations of cumulus cloud entrainment. *Atmospheric Research*, **25**, 105-127.

Lenschow, D.H., J.C. Wyngaard and W.T. Pennell, 1980: Mean-field and second moment budgets in a baroclinic convective boundary layer. *J. Atmos. Sci.*, **37**, 1313-1326.

Lock, A.P. 1998: The parametrization of entrainment in cloudy boundary layers. *Quart. J. Roy. Met. Soc.*, **124**, 2729-2753.

MacVean, M.K. and P.J. Mason, 1990: Cloud-top entrainment instability through small scale mixing and its parametrization in numerical models. *J. Atmos. Sci.*, **47**, 1012-1030.

Moeng, C-H, 2000: Entrainment rate, cloud fraction, and liquid water path of PBL Stratocumulus clouds. *J. Atmos. Sci.*, **57**, 3627-3643

Nicholls, S., 1984: The dynamics of stratocumulus: aircraft observations and comparison with a mixed-layer model. *Quart. J. Roy. Met. Soc.*, **110**, 783-820.

Nicholls, S. and J. Leighton,1986: An observational study of stratiform cloud sheets. Part I: Structure. *Quart. J. Roy. Met. Soc.*, **112**, 431-460.

Nicholls, S. and J.D. Turton, 1986: An observational study of the structure of stratiform cloud sheets: Part II Entrainment. *Quart. J. Roy. Met. Soc.*, **112**, 461-480.

Nicholls, S.,1989: The structure of radiatively driven convection in stratocumulus. *Quart. J. Roy. Met. Soc.*, **115**, 487-511.

Nieuwstadt, F.T.M. and P.G. Duynkerke, 1996: Turbulence in the atmospheric boundary layer. *Atmospheric Research*, **40**, 111-142.

Paluch, I.R. and D.H. Lenschow, 1991: Stratiform cloud formation in the marine boundary layer. *J. Atmos. Sci.*, **48**, 2141-2158.

Randall, D.A., 1980: Conditional instability of the first kind upside-down. *J. Atmos. Sci.*, **37**, 125-130.

Randall, D.A., Q. Shao, C-H Moeng, 1992: A second-order bulk boundary layer model. *J. Atmos. Sci.*, **49**, 1903-1923.

Roode, S.R. de, and P.G. Duynkerke, 1995: Dynamics of cumulus rising into stratocumulus as observed during the first "Lagrangian" experiment of ASTEX. *Quart. J. Roy. Met. Soc.*, **122**, 1597-1623.

Roode, S.R. de, and P.G. Duynkerke, 1997: Observed Lagrangian Transition of Stratocumulus into Cumulus during ASTEX: Mean State and Turbulence Structure. *J. Atmos. Sci.*, **54**, 2157-2173

Roode, S.R. de, P.G. Duynkerke and A.P. Siebesma, 2000: Analogies between mass-flux and Reynolds-averaged equations. *J. Atmos. Sci.*, **57**, 1585-1598.

Schumann, U. and C.H. Moeng, 1991: Plume fluxes in clear and cloudy boundary layers. *J. Atmos. Sci.*, **48**, 1758-1770.

Siebesma, A.P. and J.W.M. Cuijpers, 1995: Evaluation of parametric assumptions for shallow cumulus convection. *J. Atmos. Sci.*, **52**, 650-666.

Siebesma, A.P. and A.A.M. Holtslag, 1996: Model impacts of entrainment and detainment rates in shallow cumulus convection. *J. Atmos. Sci.*, **53**, 2354-2364.

Siebesma, A.P., 1996: On the mass flux approach for atmospheric convection. In: ECMWF Workshop Proceedings, 4-7 November 1996, Shinfield Park, Reading, RG2 9AX, UK.

Siems, S.T., C.S. Bretherton, M.B. Baker, S. Shy and R.E. Breidenthal, 1990: Buoyancy reversal and cloud top entrainment instability. *Quart. J. Roy. Met. Soc.*, **116**, 705- 739.

Smith, S.A. and P.R. Jonas, 1995: Observations of the turbulent fluxes in fields of cumulus clouds. *Quart. J. Roy. Met. Soc.*, **121**, 1185-1208.

Sommeria, G., 1976: Three-dimensional simulation of turbulent processes in an undisturbed trade boundary layer. *J. Atmos. Sci.*, **33**, 216-241.

Tiedtke M., 1989: A comprehensive mass flux scheme for cumulus parametrization in large-scale models. *Mon. Wea. Rev.*, **177**, 1779-1800.

VanZanten, M.C., P.G. Duynkerke and J.W.M. Cuijpers, 1998: Entrainment in convective boundary layers. *J. Atmos. Sci.*, **56**, 813-828.

Warner, J., 1977: Time variation of updraft and water content in small cumulus clouds. *J. Atmos. Sci.*, **34**, 1306-1312.

Wyngaard, J.C. and C.H. Moeng, 1992: Parameterizing turbulent diffusion through the joint probability density. *Boundary -Layer Meteor.*, **60**, 1-13.